UC Santa Barbara
UC Santa Barbara Previously Published Works

Title
A soft robot that navigates its environment through growth

Permalink
https://escholarship.org/uc/item/3nx45751

Journal
Science Robotics, 2(8)

ISSN
2470-9476

Authors
Hawkes, Elliot W
Blumenschein, Laura H
Greer, Joseph D
et al.

Publication Date
2017-07-19

DOI
10.1126/scirobotics.aan3028

Peer reviewed

eScholarship.org Powered by the California Digital Library
University of California

SOFT ROBOTS

A soft robot that navigates its environment through growth

Elliot W. Hawkes,[1,2,*] Laura H. Blumenschein,[2] Joseph D. Greer,[2] Allison M. Okamura[2]

Copyright © 2017 The Authors, some rights reserved; exclusive licensee American Association for the Advancement of Science. No claim to original U.S. Government Works

Across kingdoms and length scales, certain cells and organisms navigate their environments not through locomotion but through growth. This pattern of movement is found in fungal hyphae, developing neurons, and trailing plants, and is characterized by extension from the tip of the body, length change of hundreds of percent, and active control of growth direction. This results in the abilities to move through tightly constrained environments and form useful three-dimensional structures from the body. We report a class of soft pneumatic robot that is capable of a basic form of this behavior, growing substantially in length from the tip while actively controlling direction using onboard sensing of environmental stimuli; further, the peak rate of lengthening is comparable to rates of animal and robot locomotion. This is enabled by two principles: Pressurization of an inverted thin-walled vessel allows rapid and substantial lengthening of the tip of the robot body, and controlled asymmetric lengthening of the tip allows directional control. Further, we demonstrate the abilities to lengthen through constrained environments by exploiting passive deformations and form three-dimensional structures by lengthening the body of the robot along a path. Our study helps lay the foundation for engineered systems that grow to navigate the environment.

INTRODUCTION

Growth as a method for navigating the environment is found in fungal hyphae with diameters as small as a few micrometers (*1*) as well as in vines with girths as large as a meter (*2*–*4*). These organisms grow from their tips, increase length hundreds of times, and continually control growth direction based on environmental stimuli. Because lengthening from the tip, or apical extension, involves no relative movement of the body with respect to the environment, the body can lengthen along constrained paths without friction from sliding against the environment (Fig. 1A). Further, because each movement of the tip results in a directionally controlled lengthening of the body, the body forms into a three-dimensional (3D) structure along the path of the tip. These capabilities enable natural cells and organisms to grow through tightly packed tissue or abiotic materials and form structures with functions ranging from signal pathways to conduits for delivery (Fig. 1B) (*5*–*7*).

Although roboticists have successfully recreated movement through the environment using locomotion, defined as the translation of the body from one location to another (*8*)—flying (*9*), running (*10*), swimming (*11*, *12*), cytoplasmic streaming (*13*), slithering (*14*), and leaping (*15*)—navigating the environment through growth is challenging in artificial systems. The work on soft continuum manipulators (*16*–*20*) and tendril-like robots (*21*, *22*) has laid a foundation that has been built upon by the recent development of root-inspired robots and endoscopes that either enter a new part of the environment without changing length (*23*, *24*) or extend one to five body lengths by adding material at rates of 1 to 10 mm/min to move through granular media (*25*, *26*). However, tip-based length change on the order of thousands of percent with directional control at rates comparable to those of animal locomotion is still an open challenge.

We describe two principles that help enable a basic recreation of this behavior in an artificial system. First, an inverted, compliant, thin-walled vessel will lengthen from the tip by everting when pressurized. We present our implementation of this principle, and report results showing lengthening at the tip with length change of thousands of percent, and speeds comparable to animal locomotion. Second, the tip of the vessel steers along a path when the relative lengths of the sides of the vessel are controlled while everting. We present our implementation of this principle and show results of a soft robot lengthening toward a light, autonomously controlling direction with feedback from an onboard camera at the tip. Last, we show examples of the abilities of this type of robot body, demonstrating navigation through constrained environments and the formation of structures from the lengthening body.

RESULTS

The first principle, which is based on the eversion of a thin membrane driven by internal pressure, enables lengthening at the tip with substantial elongation and at a relatively high speed. The internal pressure forces the inverted material to evert at the tip while pulling more material from the base through the core of the body (Fig. 2A). This principle is used to deploy invaginated appendages by a variety of invertebrates such as the *Sipunculus nudus*, which everts a proboscis for defense (*27*). An analog of this method of lengthening, continuous eversion as found in cytoplasmic streaming, is the inspiration for robotic whole-skin locomotion (*13*). In our system, we implement the principle with a thin membrane of polyethylene driven by a pneumatic pump that pressurizes the interior of the soft robot body (Fig. 2, A and B, and movie S1). The design is scalable; wall stresses remain constant during geometric scaling of a thin-walled vessel, meaning that the ratio of wall thickness to diameter can be maintained. We have tested diameters ranging from 1.8 mm to 36 cm (some shown in movies S3 and S4). The thin-walled, pressurized design enables not only lengthening at the tip but also substantial length change: Very little volume of precursor wall material results in a very large volume of pressurized body. Further, unlike lengthening invertebrates, we store the precursor material in a spool, allowing length change to be

[1]Department of Mechanical Engineering, University of California, Santa Barbara, CA 93106, USA. [2]Department of Mechanical Engineering, Stanford University, Stanford, CA 94305, USA.
*Corresponding author. Email: ewhawkes@engineering.ucsb.edu

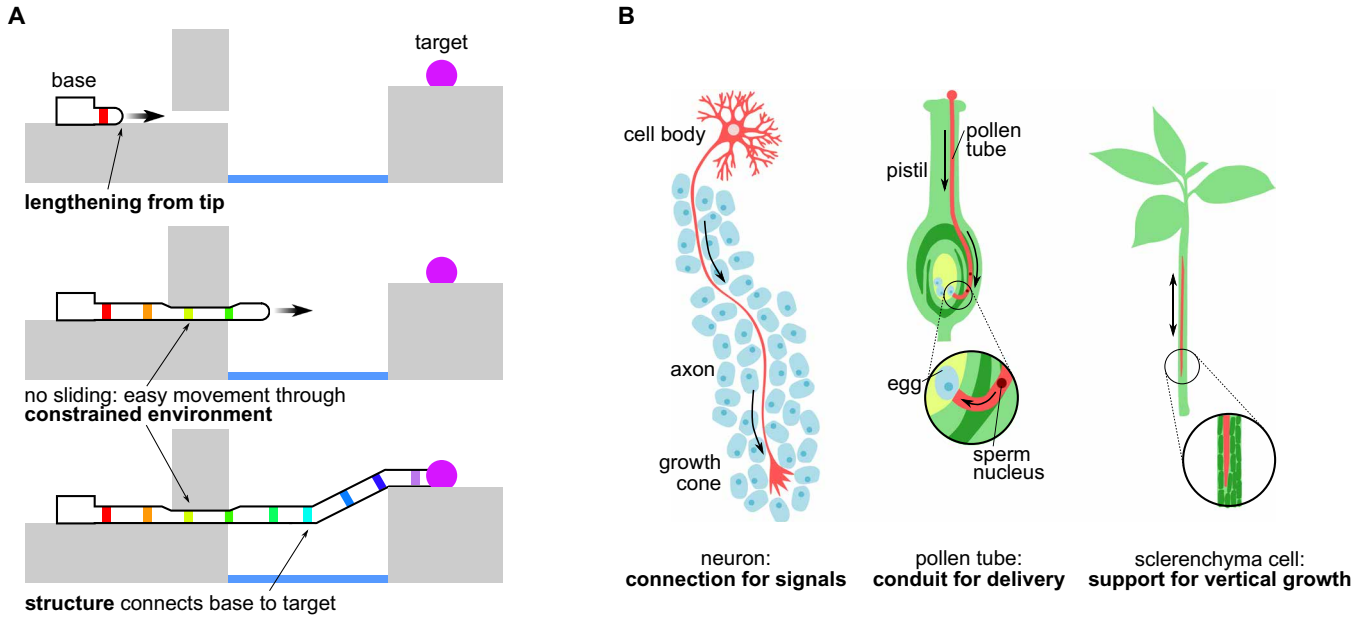

Fig. 1. Substantial lengthening from the tip with directional control enables a body to pass through a constrained environment and create a structure along its path of growth. (**A**) A body lengthens from its tip toward a target. Because only the tip moves, there is no relative movement of the body with respect to the environment (colored bands do not move). This results in the capability to move with no sliding friction through a constrained environment. As the tip moves, the body forms into a structure in the shape of the tip's path. (**B**) Examples of biological systems that grow to navigate their environments. Neurons grow through constrained tissue to create structures that act as signal pathways. Pollen tubes lengthen through pistil tissue to build conduits to deliver sperm to the ovary. Sclerenchyma cells grow within the xylem and phloem to create supporting structures.

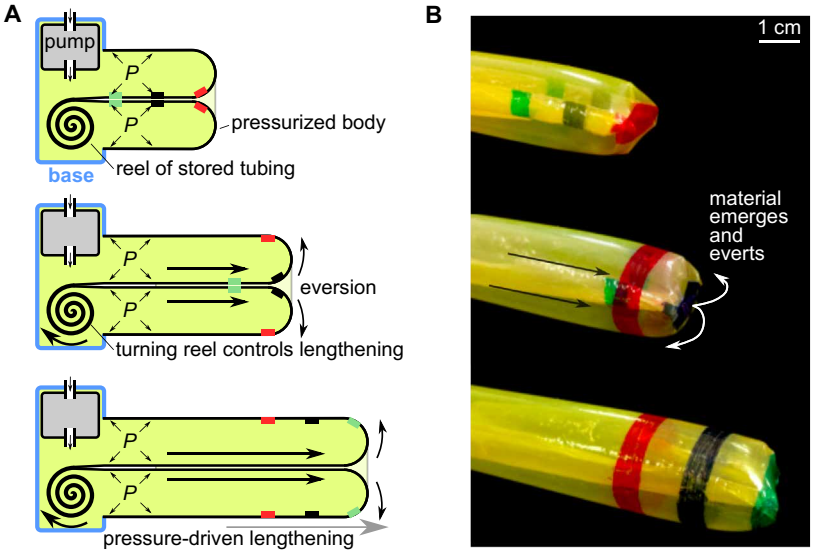

Fig. 2. Principle of pressure-driven eversion enables lengthening from the tip at rates much higher than those found in plant cell growth. (**A**) Implementation of principle in a soft robot. A pump pressurizes the body, which lengthens as the material everts at the tip. This material, which is compacted and stored on a reel in the base, passes through the core of the body to the tip; the rotation of the reel controls the length of the robot body. (**B**) Images of the lengthening body. The body diameter is 2.5 cm. (**C**) The relationship between lengthening rate (r) and internal pressure (P) shows a characteristic viscoplastic behavior: no extension below a yield pressure (Y) followed by a monotonic relationship between rate and pressure with a power term (n) close to 1. (**D**) Data show the relationship between rate and pressure above yield for the soft robot, worms with an everting proboscis (*S. nudus*), and a plant cell (*Nitella mucronata*). The extensibility φ (inverse viscosity) of a soft robot body is roughly seven orders of magnitude higher than that of the plant cell, resulting in a lengthening rate that is roughly five orders of magnitude higher. The extensibility of the soft robot body is slightly higher than the worm, which uses the same principle for lengthening.

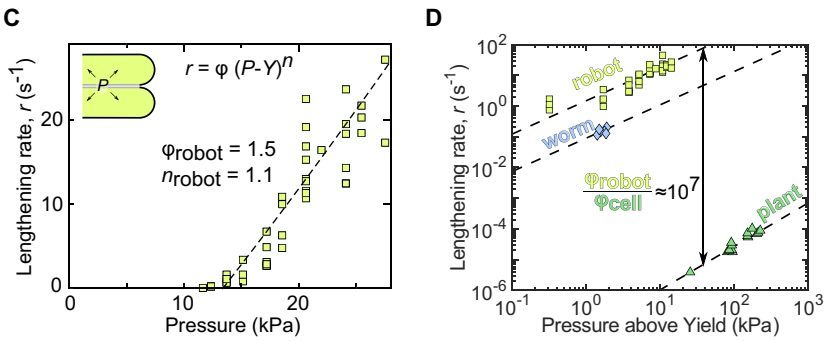

much greater than the 100% length change seen in these creatures. Although the number of turns that the soft robot body makes affects the maximum length (Supplementary Text and fig. S2), on paths with only a few turns, our system, initially 28 cm, has extended to a length of 72 m, limited by the amount of the plastic membrane on the spool (movie S1).

This principle of lengthening based on pressure-driven eversion also results in relatively fast lengthening, especially when compared to organisms that use growth to

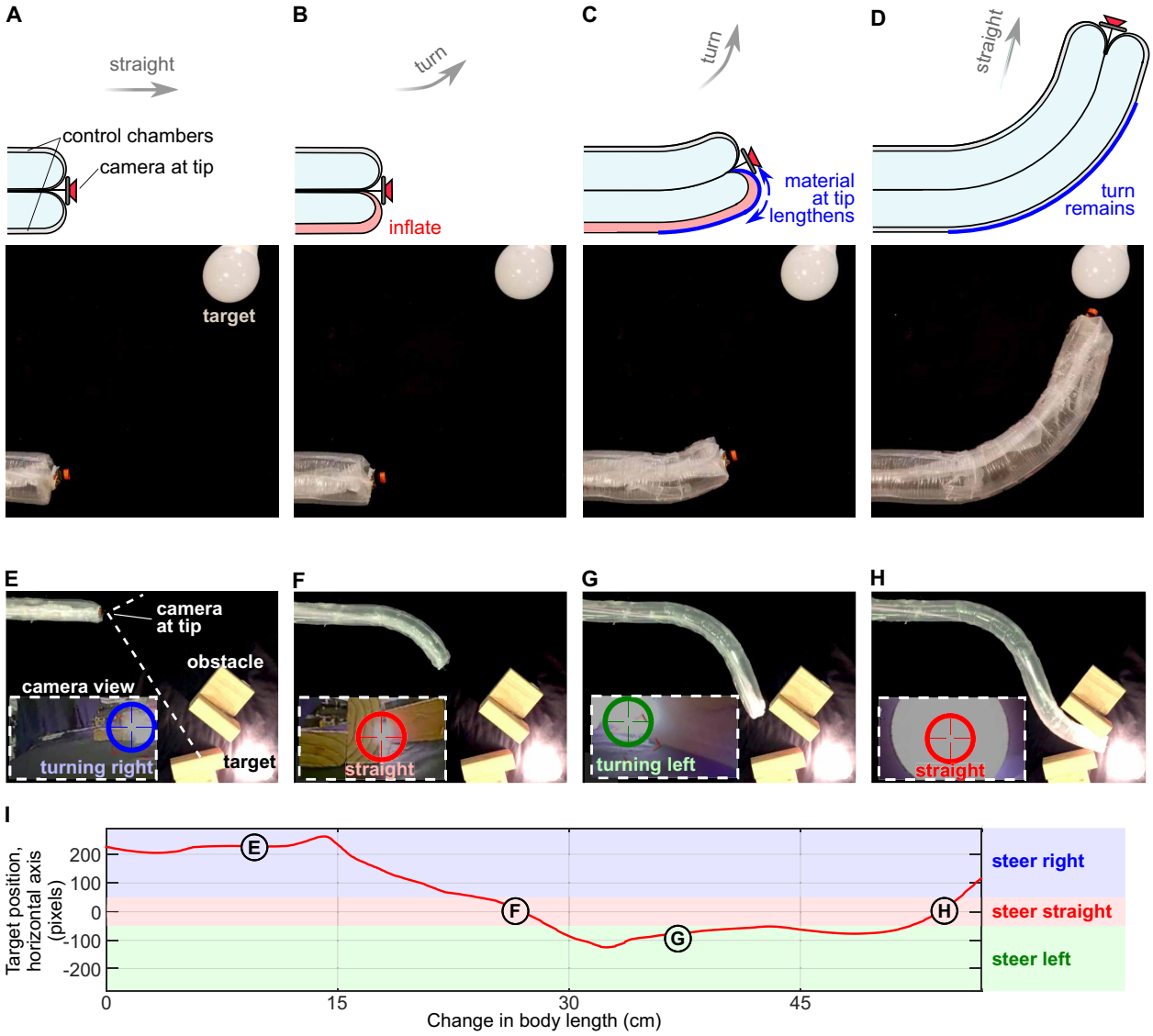

Fig. 3. Principle of asymmetric lengthening of tip enables active steering. (**A**) Implementation in a soft robot uses small pneumatic control chambers and a camera mounted on the tip for visual feedback of the environment. The camera is held in place by a cable running through the body of the robot. (**B**) To queue an upward turn, the lower control chamber is inflated. (**C**) As the body grows in length, material on the inflated side lengthens as it everts, resulting in an upward turn (see Materials and Methods and Fig.5 for details). (**D**) Once the chamber is deflated, the body again lengthens along a straight path, and the curved section remains. (**E**) A soft robot can navigate toward light using a tip-mounted camera. Inset: The view from the camera shows the target to the right. Electronically controlled solenoid valves inflate the control chamber on the left side of the robot body, resulting in the tip reorienting to the right and forming a right turn. (**F**) The target is straight ahead, and the robot steers straight. (**G**) The target is to the left, and the robot steers left. (**H**) The robot reaches the target. (**I**) Position of the target along the horizontal axis of the camera as the robot lengthens toward the target.

navigate their environments, such as certain fungi and plants. To understand the behavior of the rate of lengthening in our system, we measured the rate as we varied the internal pressure (Fig. 3C). Because of the energy losses caused by everting the membrane, we see a behavior characteristic of a Bingham plastic, in which there is a minimum required pressure before yield, and a monotonic relationship between the rate of lengthening and pressure (*28*). This is the same behavior observed in growing plant cells, which soften and then stretch because of internal pressure before new material is added to rethicken the walls (*29*–*32*). In plants, the relationship between rate and pressure is described using an inverse viscosity, termed "extensibility," φ (fig. S5; see Supplementary Text for discussion) (*33*, *34*). Our system has an extensibility that is seven orders of magnitude higher than in plants and only one order of magnitude higher than in invertebrates that use the same mechanism of lengthening (Fig. 3, C and D). Our peak bursting pressure is lower than that in a plant cell, resulting in a maximum rate of lengthening roughly five orders of magnitude higher than that in plant cells, with a maximum speed over short distances of 10 m/s. Although our implementation allows for considerably faster tip movement than that of natural cells, real-time branching, as seen in fungal hyphae in a mycelium (*1*, *35*), is not currently possible. However, a handful of preset branches are possible (fig. S4), and because the robot body is inexpensive and disposable, many

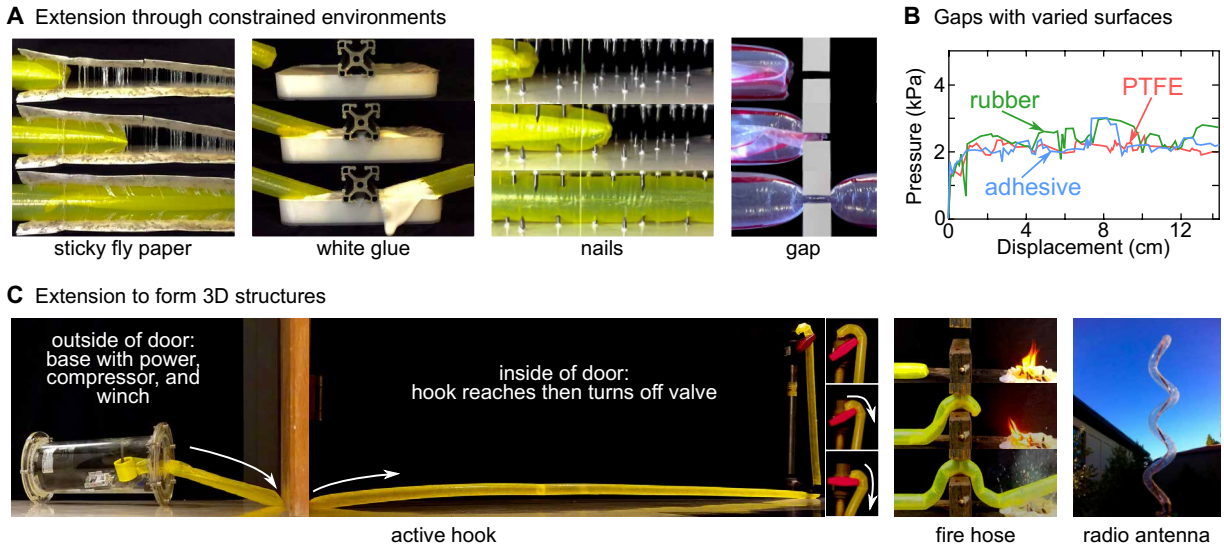

Fig. 4. Growth enables a soft robot to move its tip through constrained environments and to form 3D structures defined by the path of its tip. (**A**) A soft robot lengthens through various challenging constrained environments without active control. Instead, the robot passively deforms to navigate the obstacles. Yellow bodies, 2.5-cm diameter; clear bodies, 8-cm diameter. (**B**) The pressure required to lengthen through the gap remains relatively constant, despite vastly different surface properties of the material surrounding the gap and different displacements within the gap. Setup is shown in fig. S1. (**C**) The soft robot demonstrates the ability to lengthen into useful 3D structures.

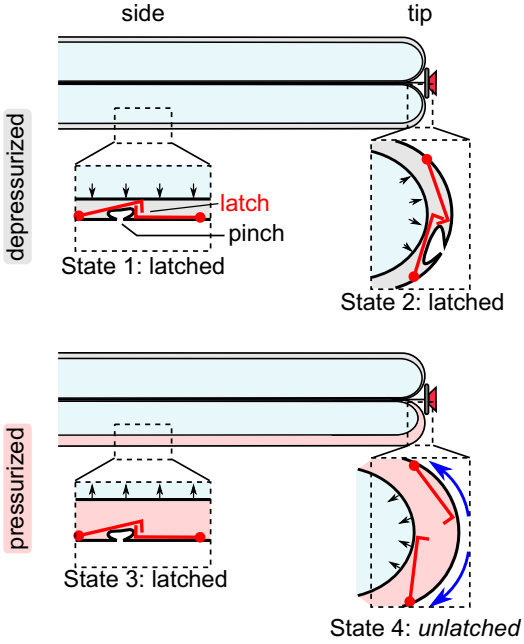

Fig. 5. Details of an implementation of a mechanism within the control chambers for selective lengthening of the sides of the soft robot. A series of latches are manufactured into the control chambers shown in Fig.3 (A to D). Each latch crosses pinched material, such that when released, the side lengthens. There are four total states. State 1: When the control chamber is depressurized and the latch is on the side, the latch remains closed. State 2: When the control chamber is depressurized and the latch is at the tip, the latch remains closed. (When a control chamber is depressurized, the pressure from the main chamber keeps the latch closed regardless of whether the latch is on the side or at the tip.) State 3: When the control chamber is pressurized and the latch is on the side, the latch remains closed. State 4: When the control chamber is pressurized and the latch is at the tip, the latch opens. (When the control chamber is pressurized, the latch remains closed if it is along a side, due to the shape of the interlocking of the latch, but the latch opens if it is at the tip because the high curvature overcomes the interlocking.)

parallel bodies, like a single branched body, could cover large areas for search and rescue applications (see Materials and Methods for manufacturing details).

The second principle that we leverage in our design enables the active control of direction and is based on setting the relative lengths of either side of the body at the tip as the body grows in length. This principle of directional control is found in tip-growing cells such as pollen tubes (*36*), fungal hyphae (*1*), rhizoids of algae (*37*), and root hairs (*7*). In our system, we implement this principle by selectively allowing one side of the robot body to lengthen with respect to the other side as the body everts from the tip (Fig. 3, A to D). Small control chambers that run along the side of the robot body act as the control input; when one of these chambers is inflated, the section of the robot body that is everting from the tip on that side will be lengthened. For example, when the left channel is inflated, the left side of the tip lengthens, resulting in a right turn (see Materials and Methods and Fig. 5 for details). Thus, by controlling the relative pressures of these control chambers, steering is achieved (movie S2). This method of turning is efficient and simple; it requires neither the addition of energy (beyond the control signal) nor any bulky actuators to bend an existing segment. Rather the turn is created at the same time as the segment, using the energy stored in the pressurized fluid of the main chamber. Each turn is permanent, thus control of direction is nonholonomic (*38*), like in a steering car or growing pollen tube. Our implementation results in much faster changes in direction than the chemical diffusion of natural cells [less than a second for our system in contrast to roughly a minute for pollen tubes (*39*)]. However, our implementation has closely packed discrete sections that can be lengthened (Fig. 5), resulting in a digital system, which sacrifices some resolution that an analog system affords. To demonstrate our implementation, a soft robot navigates to a light using an onboard tip-mounted camera with closed-loop active control (Fig. 3, E to H, and movie S2).

In addition to demonstrating tip growth, substantial length increase, high-speed tip motion, and directional control, the presented class of

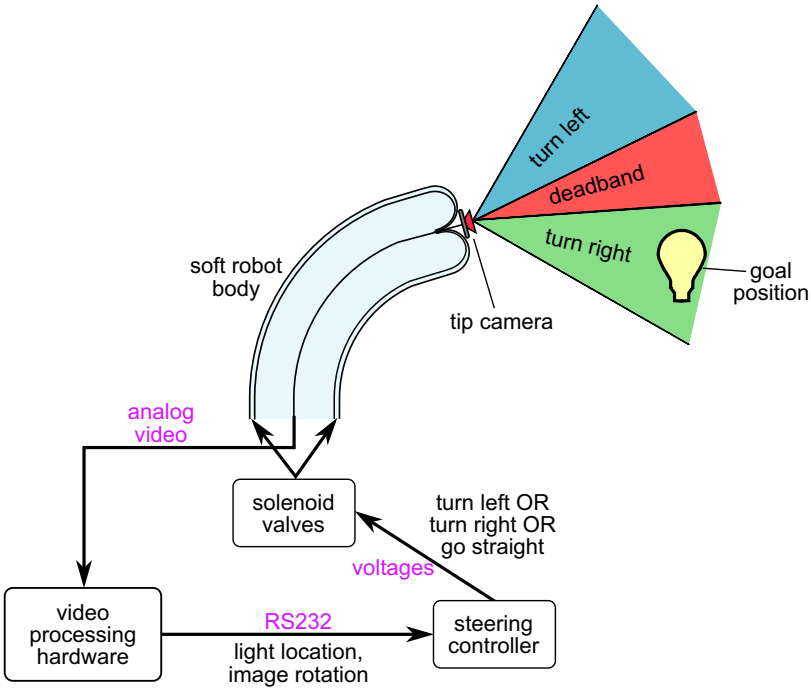

Fig. 6. Overview of active steering control system. Hardware components and a physical depiction of the steering task are shown. Electrical signal formats are labeled in purple, and their semantic meanings are labeled in black.

soft robot shows some of the capabilities of natural cells and organisms that navigate by growth: movement through tightly constrained environments and the creation of 3D structures with the lengthening body. We tested our system by lengthening a soft robot body through challenging constrained environments (Fig. 4A and movie S3) and demonstrated its insensitivity to surface characteristics (Fig. 4B): It takes no more pressure to grow between two adhesive surfaces than between two polytetrafluoroethylene (PTFE) surfaces. Its ability to passively deform aids in its ability to move through constrained spaces and adapt to the environment. We also demonstrated 3D structures created by lengthening a preformed body: an active hook, a fire hose, and a radio antenna (Fig. 4C and fig. S3), as well as a structure that lengthens across land and water and another that pulls a cable through a dropped ceiling (movie S4). Like the natural examples of structure creation (Fig. 1B), a variety of purposes are demonstrated: the fire hose demonstrates delivery (like pollen tubes), the structure of the antenna demonstrates support (like sclerenchyma cells), and the cable-pulling structure demonstrates connecting remote locations (like neurons).

CONCLUSION

Growth is an intriguing method for navigating the environment and is found across kingdoms and scales in nature. Although limited in range, it allows access to constrained environments and enables the creation of 3D structures along the path of movement. We demonstrated basic versions of these capabilities in a class of pressure-driven soft robot and presented robot bodies that range across two orders of magnitude in diameter. This type of robot body can lengthen by thousands of percent from its tip, and its peak rate of extension is comparable to that of animal or robot locomotion. Further, we demonstrated active control of direction with onboard sensing, enabling response to an environmental stimulus. Our results help pave the way for engineered systems to exploit growth as a paradigm for navigating constrained environments while forming potentially useful 3D structures.

MATERIALS AND METHODS

Construction

A lengthening soft robot comprises two main components: the extending body and the base (Fig. 2A). Along the length of the extending body are control chambers that can be selectively inflated by the solenoid valves. There are chambers along two sides (for creating 2D shapes during lengthening) or three sides (for creating 3D shapes during extension). When a chamber is inflated during lengthening, the material at the tip of the inflated control chamber side lengthens. This creates a turn in the direction away from the inflated control chamber (Fig. 3, A to D).

Although a variety of implementations can realize this behavior, we describe the one used for the robot shown in Fig. 3. Within each control chamber is a continuous row of latches, with each latch roughly 2 cm long (body diameter is 3.8 cm). Each engaged latch crosses pinched wall material; in this way, the side lengthens when the latch is opened without requiring the material to stretch (Fig. 5). The opening of the latches is controlled by the pressure in its control chamber as well as the location of the latch. When a control chamber is not pressurized, the pressure from the main chamber keeps the latches closed. However, when the control chamber is pressurized, a latch can open, but only if it is at the tip of the robot body. When at the tip, the curvature causes the latch to release and the section to lengthen. In contrast, if the latch is on a straight section, it remains closed because of the interlocking of the latch. The latches are manufactured from a combination of sheet steel and polypropylene and attached to the outer wall using a soft viscoelastic adhesive (TrueTape LLC). The latches can also be produced by 3D printing for large-batch fabrication. The latches can be reset after lengthening for a reusable system.

The change in the steering angle θ that a single closed latch will cause can be described by $\theta = \frac{l}{d}$, where l is the length removed by the pinch and d is the diameter of the robot body. This relationship is derived by assuming that the pinched and unpinched sides of the robot body lie on concentric circles, with the body diameter being the difference in the radius between the two curves.

The other component of the robot is the base. One implementation of the base (shown in Fig. 4C) is a cylindrical airtight acrylic vessel (28 cm long, 18 cm in diameter), containing a 6-V battery-powered air compressor (Ingersoll Rand B01HG0FTAM) that crosses the vessel boundary. Note that most testing was done with an off-board air supply. When turned on, the compressor increases the mass of the air inside the vessel, resulting in a force that tends to lengthen the robot body. A spool of thin-walled polyethylene tubing (50- to 80-μm wall thickness; Elkay Plastics) supplies new material for lengthening, and a winching motor (Maxon) can control the rate and the direction that the spool turns. Electronically controlled solenoid valves selectively pressurize the control chambers of the robot body.

Active steering control with onboard sensing

A simple task was created to demonstrate real-time steering control of the soft robot using onboard sensing. The objective of the task was

to steer the tip of the soft robot in two dimensions to a goal location, indicated by an illuminated light bulb (Fig. 6).

Hardware overview

The location of the illuminated light bulb was sensed using a miniature analog camera (640 × 480, 30 frames/s) at the tip of the soft robot. The camera's cables were routed along the inside of the robot's body, and the camera was kept at the tip by applying a constant tension force to its cables. This also served as a limit to the extension rate of the robot. Air was supplied to the main chamber of the soft robot with a pressure regulator. As described above and in Fig. 3, steering was implemented by inflating the control chambers of the robot: To turn right, the left chamber is inflated; to turn left, the right chamber is inflated; and to go straight, both side chambers (or neither chamber) are inflated. Electronic solenoids were used to selectively inflate the side chambers based on the commands of the vision-based steering controller.

Vision processing

Data from the tip camera were processed using specialized video processing hardware (SLA-2000, Sightline Applications Inc.). The video processing hardware computed both the location of the light and camera rotation about its optical axis. Light location was calculated using template-based object tracking, and camera rotation was calculated using image registration between the current and the last frame. Light location (in pixels) and camera rotation (in degrees) were communicated to the steering controller via RS-232.

Steering controller

The soft robot was controlled to steer toward the light using a bang-bang heading controller that aligned the robot's tip heading with the ray emanating from the robot's tip to the light (Fig. 6). The light location, computed by the video processing hardware, was used to make decisions about when to turn left, turn right, or go straight. A 100-pixel deadband was designated in the center of the tip camera frame. If the light location was more than 50 pixels to the left or right of the center of the tip camera image, then the steering controller commanded a left or right turn, respectively. Otherwise, the robot was commanded to go straight. Camera rotation relative to the robot body was estimated by integrating frame-to-frame rotation information. The estimated rotation was used to transform the location of the light into the robot coordinate frame so that a left-right steering decision could be made.

SUPPLEMENTARY MATERIALS

robotics.sciencemag.org/cgi/content/full/2/8/eaan3028/DC1

Text

Fig. S1. Experimental arrangement for collection of data shown in Figs.2 and 4 and fig. S2.

Fig. S2. Additional experimental results from tests to determine full model for soft robot lengthening.

Fig. S3. Modeling of a helical antenna formed with a soft robot.

Fig. S4. Extension of a soft robot body with preset pattern of branching.

Fig. S5. Viscoplastic relationships for natural extending systems.

Movie S1. Lengthening.

Movie S2. Steering.

Movie S3. Constrained environments.

Movie S4. Forming structures from the body.

References (*40*, *41*)

REFERENCES AND NOTES

1. R. R. Lew, How does a hypha grow? The biophysics of pressurized growth in fungi. *Nat. Rev. Microbiol.* **9**, 509–518 (2011).
2. D. Weigel, G. Jürgens, Stem cells that make stems. *Nature* **415**, 751–754 (2002).
3. K. C. Vaughn, A. J. Bowling, Biology and physiology of vines. *Hortic. Rev.* **38**, 1–21 (2011).
4. Historical Royal Palaces, The Great Vine; www.hrp.org.uk/hampton-court-palace/visit-us/top-things-to-see-and-do/the-great-vine.
5. E. W. Dent, F. B. Gertler, Cytoskeletal dynamics and transport in growth cone motility and axon guidance. *Neuron* **40**, 209–227 (2003).
6. R. Palanivelu, D. Preuss, Pollen tube targeting and axon guidance: Parallels in tip growth mechanisms. *Trends Cell Biol.* **10**, 517–524 (2000).
7. A. S. Nezhad, A. Geitmann, The cellular mechanics of an invasive lifestyle. *J. Exp. Bot.* **64**, 4709–4728 (2013).
8. R. M. Alexander, *Principles of Animal Locomotion* (Princeton Univ. Press, 2003).
9. K. Y. Ma, P. Chirarattananon, S. B. Fuller, R. J. Wood, Controlled flight of a biologically inspired, insect-scale robot. *Science* **340**, 603–607 (2013).
10. S. Seok, A. Wang, M. Y. Chuah, D. Jin Hyun, J. Lee, D. M. Otten, J. H. Lang, S. Kim, Design principles for energy-efficient legged locomotion and implementation on the MIT Cheetah Robot. *IEEE/ASME Trans. Mechatronics* **20**, 1117–1129 (2015).
11. Z. Wang, G. Hang, J. Li, Y. Wang, K. Xiao, A micro-robot fish with embedded SMA wire actuated flexible biomimetic fin. *Sensor. Actuat. A Phys.* **144**, 354–360 (2008).
12. A. D. Marchese, C. D. Onal, D. Rus, Autonomous soft robotic fish capable of escape maneuvers using fluidic elastomer actuators. *Soft Robot.* **1**, 75–87 (2014).
13. D. W. Hong, M. Ingram, D. Lahr, Whole skin locomotion inspired by amoeboid motility mechanisms. *J. Mech. Robot.* **1**, 011015 (2008).
14. H. Marvi, C. Gong, N. Gravish, H. Astley, M. Travers, R. L. Hatton, J. R. Mendelson III, H. Choset, D. L. Hu, D. I. Goldman, Sidewinding with minimal slip: Snake and robot ascent of sandy slopes. *Science* **346**, 224–229 (2014).
15. J.-S. Koh, E. Yang, G.-P. Jung, S.-P. Jung, J. H. Son, S.-I. Lee, P. G. Jablonski, R. J. Wood, H.-Y. Kim, K.-J. Cho, Jumping on water: Surface tension–dominated jumping of water striders and robotic insects. *Science* **349**, 517–521 (2015).
16. J. F. Wilson, D. Li, Z. Chen, R.T. George Jr., Flexible robot manipulators and grippers: Relatives of elephant trunks and squid tentacles, in *Robots and Biological Systems: Toward a New Bionics?* P. Dario, G. Sandini, P. Aebischer, Eds. (Springer, 1993), pp. 474–479.
17. G. Immega, K. Antonelli, The KSI tentacle manipulator, in *Proceedings of 1995 IEEE International Conference on Robotics and Automation (IROS)* (IEEE, 1995), pp. 3149–3154.
18. R. Cieslak, A. Morecki, Elephant trunk type elastic manipulator—A tool for bulk and liquid type materials transportation. *Robotica* **17**, 11–16 (1999).
19. H. Tsukagoshi, A. Kitagawa, M. Segawa, Active hose: An artificial elephant's nose with maneuverability for rescue operation, in *Proceedings of the IEEE International Conference on Robotics and Automation (IROS)* (IEEE, 2001), pp. 2454–2459.
20. W. McMahan, B. A. Jones, I. D. Walker, Design and implementation of a multi-section continuum robot: Air-octor, in *Proceedings of the IEEE/RSJ International Conference on Intelligent Robots and Systems (IROS)* (IEEE, 2005), pp. 2578–2585.
21. J. S. Mehling, M. A. Diftler, M. Chu, M. Valvo, A minimally invasive tendril robot for in-space inspection, in *Proceedings of the First IEEE/RAS-EMBS International Conference on Biomedical Robotics and Biomechatronics (BioRob)* (IEEE, 2006), pp. 690–695.
22. M. B. Wooten, I. D. Walker, A novel vine-like robot for in-orbit inspection, in *Proceedings of the 45th International Conference on Environmental System* (ICES, 2015), pp. 1–11.
23. A. Sadeghi, A. Tonazzini, L. Popova, B. Mazzolai, Robotic mechanism for soil penetration inspired by plant root, in *Proceedings of the IEEE International Conference on Robotics and Automation (ICRA)* (IEEE, 2013), pp. 3457–3462.
24. T. Rösch, A. Adler, H. Pohl, E. Wettschureck, M. Koch, B. Wiedenmann, N. Hoepffner, A motor-driven single-use colonoscope controlled with a hand-held device: A feasibility study in volunteers. *Gastrointest. Endosc.* **67**, 1139–1146 (2008).
25. A. Sadeghi, A. Tonazzini, L. Popova, B. Mazzolai, A novel growing device inspired by plant root soil penetration behaviors. *PLOS ONE* **9**, e90139 (2014).
26. E. Del Dottore, A. Mondini, A. Sadeghi, V. Mattoli, B. Mazzolai, Circumnutations as a penetration strategy in a plant-root-inspired robot, in *Proceedings of the IEEE International Conference on Robotics and Automation (ICRA)* (IEEE, 2016), pp. 4722–4728.
27. E. Zuckerkandl, Coelomic pressures in Sipunculus nudus. *Biol. Bull.* **98**, 161–173 (1950).
28. E. C. Bingham, *Fluidity and Plasticity* (McGraw-Hill, 1922).
29. J. Dumais, S. L. Shaw, C. R. Steele, S. R. Long, P. M. Ray, An anisotropic-viscoplastic model of plant cell morphogenesis by tip growth. *Int. J. Dev. Biol.* **50**, 209–222 (2006).
30. A. Geitmann, M. Steer, The architectural and properties of the pollen tube cell wall, in *The Pollen Tube: A Cellular and Molecular Perspective*, R. Malhó, Ed. (Springer, 2006), pp. 177–200.
31. D. J. Cosgrove, Growth of the plant cell wall. *Nat. Rev. Mol. Cell Biol.* **6**, 850–861 (2005).
32. T. I. Baskin, Anisotropic expansion of the plant cell wall. *Annu. Rev. Cell Dev. Biol.* **21**, 203–222 (2005).
33. J. A. Lockhart, An analysis of irreversible plant cell elongation. *J. Theor. Biol.* **8**, 264–275 (1965).
34. P. B. Green, R. O. Erickson, J. Buggy, Metabolic and physical control of cell elongation rate: *In vivo* studies in *Nitella*. *Plant Physiol.* **47**, 423–430 (1971).
35. L. L. M. Heaton, E. López, P. K. Maini, M. D. Fricker, N. S. Jones, Growth-induced mass flows in fungal networks. *Proc. Biol. Sci.* **277**, 3265–3274 (2010).
36. M. W. Steer, J. M. Steer, Pollen tube tip growth. *New Phytol.* **111**, 323–358 (1989).
37. Z. Hejnowicz, B. Heinemann, A. Sievers, Tip growth: Patterns of growth rate and stress in the Chara rhizoid. *Z. Tierpsychol.* **81**, 409–424 (1977).

38. R. J. Webster III, J. S. Kim, N. J. Cowan, G. S. Chirikjian, A. M. Okamura, Nonholonomic modeling of needle steering. *Int. J. Robot. Res.* **25**, 509–525 (2006).
39. H. Takeuchi, T. Higashiyama, Tip-localized receptors control pollen tube growth and LURE sensing in *Arabidopsis*. *Nature* **531**, 245–248 (2016).
40. M. Kaneko, T. Yamashita, K. Tanie, Basic considerations on transmission characteristics for tendon drive robots, in *Proceedings of the Fifth International Conference on Advanced Robotics, Robots in Unstructured Environments (ICAR)* (IEEE, 1991), pp. 827–832.
41. A. A. Griffith, The phenomena of rupture and flow in solids. *Philos. Trans. R. Soc. Lon. A* **221**, 163–198 (1921).

Acknowledgments: We thank T. Chang, C. Lin, and J. Fan for help in designing and analyzing the antenna; D. Christensen, T. Morimoto, A. Suresh, S. Follmer, and M. Cutkosky for helpful discussions leading to design approaches; Z. Hammond, P. Slade, A. Piedra, and M. Lepert for help in designing and manufacturing soft robots; S. Sketch for input on figures; neurosurgeons G. Grant and J. Quon for consultation for potential uses in surgery; the Stanford Office of University Communications for help with filming; D. Lentink for helpful suggestions on the manuscript; and H. Bluestone for help editing. **Funding:** This work was supported in part by the NSF (grant no. 1637446) and the NSF Graduate Research Fellowship Program. **Author contributions:** E.W.H. designed the soft robot, models, and experiments and wrote the manuscript. L.H.B. designed experiments and models, performed experiments, analyzed data, and wrote the methods. J.D.G. designed the controller and performed experiments. A.M.O. directed the project, defined the analysis, and edited the manuscript. **Competing interests:** E.W.H. and A.M.O. have a provisional patent application on the method of lengthening. **Data and materials availability:** All data are provided in the manuscript and the Supplementary Materials.

Submitted 24 March 2017
Accepted 23 June 2017
Published 19 July 2017
10.1126/scirobotics.aan3028

Citation: E. W. Hawkes, L. H. Blumenschein, J. D. Greer, A. M. Okamura, A soft robot that navigates its environment through growth. *Sci. Robot.* **2**, eaan3028 (2017).

Abstract

One-sentence summary: A class of soft robot can substantially and rapidly increase length from its tip and steer to navigate its environment.